Table I. Rate of Ion Transport

	k_{rel}		k_{rel}
Hg^{2+}	200.0	Cu^{2+}	0.4
Zn^{2+}	1.0	Ca^{2+}	0.1
Cd^{2+}	1.0		

outlined in Figure 1. A barrier was placed between the arms of a water-jacketed U-tube, with a 100-W sun lamp (visible light source) on one side and a 350-W medium pressure mercury lamp on the other, immersed in a visible light filter solution that would cut off light with $\lambda > 350$ nm,[13] ensuring the maintenance of constant temperature while the two interfaces were separately exposed to either visible, ultraviolet, or no irradiation ($h\nu_1$ and $h\nu_2$). Four experiments were performed,[14] which are summarized in Figure 2: the metal solution–chloroform interface was irradiated with UV light, and the chloroform–H_2O interface was irradiated with visible light (UV–vis); only the chloroform–H_2O interface was irradiated with visible light (vis-enhanced); the metal solution–chloroform interface was irradiated with visible light (vis-inhibit); and no irradiation at either interface (control). Both aqueous layers had samples removed periodically, which were assayed for metal content by using atomic absorption spectroscopy. As indicated in Figure 1, the rate of transport varied from 0.005 μg/h, when visible light is used to retard metal uptake, to 0.25 μg/h when metal uptake is stimulated with UV irradiation and metal release is induced by visible light irradiation, representing a 50-fold irradiation-dependent variation in transport rate.[15]

These results are consistent with the known effect of visible and ultraviolet irradiation on the concentration of the zwitterionic species in the **3** = **4** equilibrium.[3] Irradiation of the metal solution–chloroform interface with ultraviolet light ($h\nu_1$) increases the concentration of the zwitterionic species so that more metal can be transported across the interface, while irradiation at the same interface with visible light decreases the concentration of the zwitterionic species, and even less metal is transported into the chloroform phase than in the control experiment, in which there is no irradiation at either interface. When the chloroform–water interface is irradiated with visible light ($h\nu_2$), however, the transport rate increases because visible irradiation causes release of the bound metal. The importance of the bidentate zwitterion in achieving the metal ion transport was clearly demonstrated by repeating the zinc transport experiment with **3c**, which lacks the piperidomethyl appendage on the spiropyranindoline. In this experiment, no transport was observed under any of the irradiation conditions.

The transport of other metal ions using **3b** = **4b** was examined, and the results are summarized in Table I. No transport was observed with solutions of Fe^{3+}, Co^{2+}, Ni^{2+}, or Li^{1+}, indicating that group Ib and IIb metal cations are best suited for transport using this system. While Cd^{2+} gave very similar results to those obtained with Zn^{2+}, the results obtained with Hg^{2+} were very different. Not only was the rate of transport much faster with Hg^{2+} than with other ions, but, in contrast to the zinc result described above, the rate of mercury transport was insensitive to UV irradiation at the interface of the chloroform–metal solution ($h\nu_1$). To test whether the same mode of metal binding by **3b** was operational with Hg^{2+} and Zn^{2+}, the mercury experiment was repeated with **3c**, the spiropyranindoline lacking the attached ligating group. While no transport of Zn^{2+} had been observed with **3c**, the rate of transport of Hg^{2+} with **3b** and **3c** were the same, indicating that the binding of mercury by **3b** was different than the other group IIb metal cations, possibly via a π complex, which dissociates on irradiation.[16]

In conclusion, we have demonstrated photodynamic ion transport using spiropyranindoline **3a** and the chloride salts of zinc(II), copper(II), and cadmium(II). Changes in transport rate of an order of magnitude were observed. Further studies directed toward increasing the rate of transport and the development of photodynamic active transport of metal ions across a concentration gradient are currently underway in our laboratory.

Acknowledgment. We thank Professor Brice Bosnich for valuable discussions and Dr. Andrew Davis for invaluable assistance in obtaining the atomic absorption data. Support from the Office of Naval Research and the Dow Chemical Company is gratefully acknowledged. The NMR instruments used were funded in part by the NSF Chemical Instrumentation Program and by the NCI via the University of Chicago Cancer Research Center (CA 14599).

(11) Ultraviolet spectra of a 5×10^{-5} M solution of spiropyranindoline in 1:1 acetone/ethanol in the presence of 50 equiv of metal chloride or perchlorate were monitored at 520 nm, the λ_{max} of the zwitterionic form **4** (ref 3 and 4).

(12) It was necessary to employ the decyl chain on the indoline nitrogen to prevent the zwitterionic form, **4**, from forming emulsions at the chloroform–water interface.

(13) Sunamoto, J.; Kiyoshi, K.; Yukio, M.; Tetsumi, K. *J. Am. Chem. Soc.* **1982**, *104*, 5502.

(14) The experiments were performed by charging the U-tube with 4 mL of 50 mM $ZnCl_2$, 7 mL of 3 mM spiropyranindoline in chloroform, and 4 mL of H_2O.

(15) Starting with equal concentrations of metal ion in both aqueous phases in the apparatus described in Figure 1 should result in photodynamic transport across the organic membrane, producing an increased metal ion concentration on one side and a diminished one on the other side. However, the rates of transport described in Figure 1 (μg Zn[2+]/hr) are too slow to permit the photodynamic transport of metal ion across a concentration gradient to be accurately measured using the present analytical method.

(16) For a discussion of the reversibility of the mercuration of alkenes, see: Halpern, J.; Tinker, H. B. *J. Am. Chem. Soc.* **1967**, *89*, 6427.

Heteronuclear Three-Dimensional NMR Spectroscopy. Natural Abundance ^{13}C Chemical Shift Editing of ^1H–^1H COSY Spectra

Stephen W. Fesik,* Robert T. Gampe, Jr., and Erik R. P. Zuiderweg

Pharmaceutical Discovery Division
Abbott Laboratories, D-47G, AP9
Abbott Park, Illinois 60064
Received October 7, 1988

Homonuclear three-dimensional (3D) NMR spectroscopy has been shown to be an effective means of resolving spectral overlap observed in two-dimensional (2D) NMR experiments.[1-4] By combining two proton 2D NMR experiments in which the detection period of the first experiment serves as the evolution period of the second, a proton that is frequency labeled in t_1 can be correlated to a second proton (t_2) and further correlated to a third (t_3) by using similar or different types of experiments.[2-4] We have recently shown[5] that this same principle can be applied to produce a heteronuclear 3D NMR experiment by combining a heteronuclear shift correlation and a homonuclear 2D NMR experiment (e.g., COSY, NOESY). As previously demonstrated[5] with a uniformly ^{15}N-labeled peptide, homonuclear COSY and NOESY spectra can be simplified with this technique by editing with respect to the heteronuclear chemical shifts in a third dimension. Since a large heteronuclear J coupling is involved in one of the coherence transfer steps, heteronuclear 3D NMR spectroscopy appears particularly promising in structural studies of large, isotopically labeled biomolecules.

In this communication we demonstrate that heteronuclear 3D NMR spectroscopy can also be effectively applied to small molecules with ^{13}C at natural abundance. The approach is illustrated for a 78 mM solution of the aminoglycoside, kanamycin A (structure shown in Figure 1). As for most saccharides, the

(1) Vuister, G. W.; Boelens, R. *J. Magn. Reson.* **1987**, *73*, 328.

(2) Griesinger, C.; Sorensen, O. W.; Ernst, R. R. *J. Magn. Reson.* **1987**, *73*, 574.

(3) Griesinger, G.; Sorensen, O. W.; Ernst, R. R. *J. Am. Chem. Soc.* **1987**, *109*, 7227.

(4) Oschkinat, H.; Griesinger, C.; Kraulis, P. J.; Sorensen, O. W.; Ernst, R. R.; Gronenborn, A. M.; Clore, G. M. *Nature (London)* **1988**, *332*, 374.

(5) Fesik, S. W.; Zuiderweg, E. R. P. *J. Magn. Reson.* **1988**, *78*, 588.

0002-7863/89/1511-0770$01.50/0

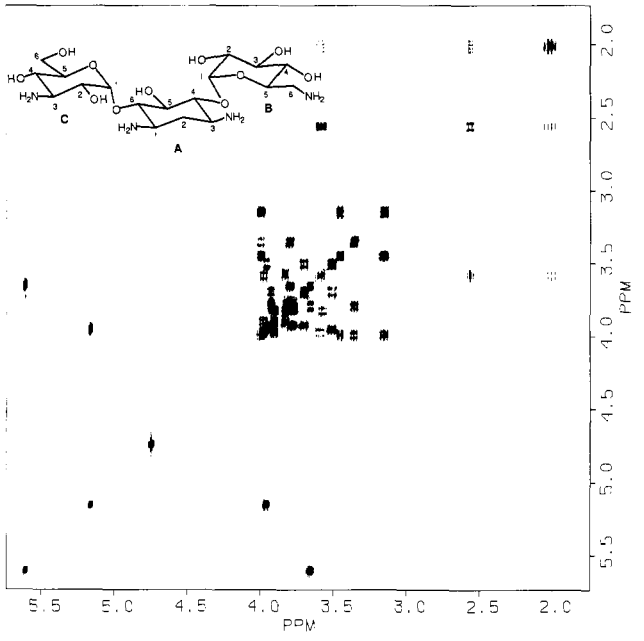

Figure 1. Phase sensitive COSY spectrum of a 78 mM solution of kanamycin A (structure shown in inset) in D_2O (pD = 2.4). Both positive and negative contours are plotted. Chemical shifts are referenced to internal sodium 3-trimethylsilyl propionate (TSP).

two-dimensional phase-sensitive COSY spectrum (Figure 1) of this aminoglycoside is quite complex in the spectral region between 3.0–4.0 ppm. However, this spectrum can be markedly simplified and thus made easier to interpret by editing with respect to the ^{13}C chemical shifts in a 3D NMR experiment.

The pulse sequence of the 3D NMR experiment is $90_x(^1H)$–τ–$90_\theta(^{13}C)$–$t_{1/2}$–$180_x(^1H)$–$t_{1/2}$–$90_x(^{13}C)$–τ–t_2–$90_\phi(^1H)$–acquire(t_3) in which θ = X, –X, X, –X, ϕ = X, X, –X, –X, and the receiver is cycled X, –X, X, –X. A bilinear (BIRD) pulse followed by a delay (0.4 s) was performed at the beginning of the sequence to enhance the suppression of the signals of the protons not coupled to ^{13}C.[7] ^{13}C decoupling was applied during t_2 and t_3 by using a Waltz-16 decoupling scheme.[8] Basically, the 3D sequence consists of a combination of a heteronuclear multiple-quantum correlation (HMQC) and a homonuclear COSY experiment in which the ^{13}C NMR signals are indirectly detected in ω_1, the protons attached to these carbons in ω_2, and the scalar coupled proton partners are observed in ω_3.

Figure 2 depicts individual planes (ω_2, ω_3) of the 3D HMQC-COSY data set corresponding to each of the ^{13}C signals (ω_1) of kanamycin A. As observed, the ^1H–^1H COSY spectrum is now spread out over many planes and is markedly simplified. Only diagonal peaks corresponding to the protons attached to the carbons resonating at the ^{13}C frequencies selected in ω_1 and cross peaks corresponding to their scalar coupled partners are observed in each plane. Since the proton signals that are detected in ω_2 can only originate from an attached carbon, the 3D data is asymmetric about the diagonal in the individual ω_2, ω_3 planes. This type of pattern is expected from the coherence transfer pathway [($^{13}C(t_1)$→$^{13}CH(t_2)$→$^{13}CH(t_3)$ + scalar coupled protons (t_3)] chosen in the experiment.

In order to analyze the 3D data, the scalar coupled protons are identified within a particular ^{13}C plane (horizontal lines in Figure 2), followed by the selection of new planes (vertical lines) which contain a particular pattern of signals.[9] As illustrated for ring

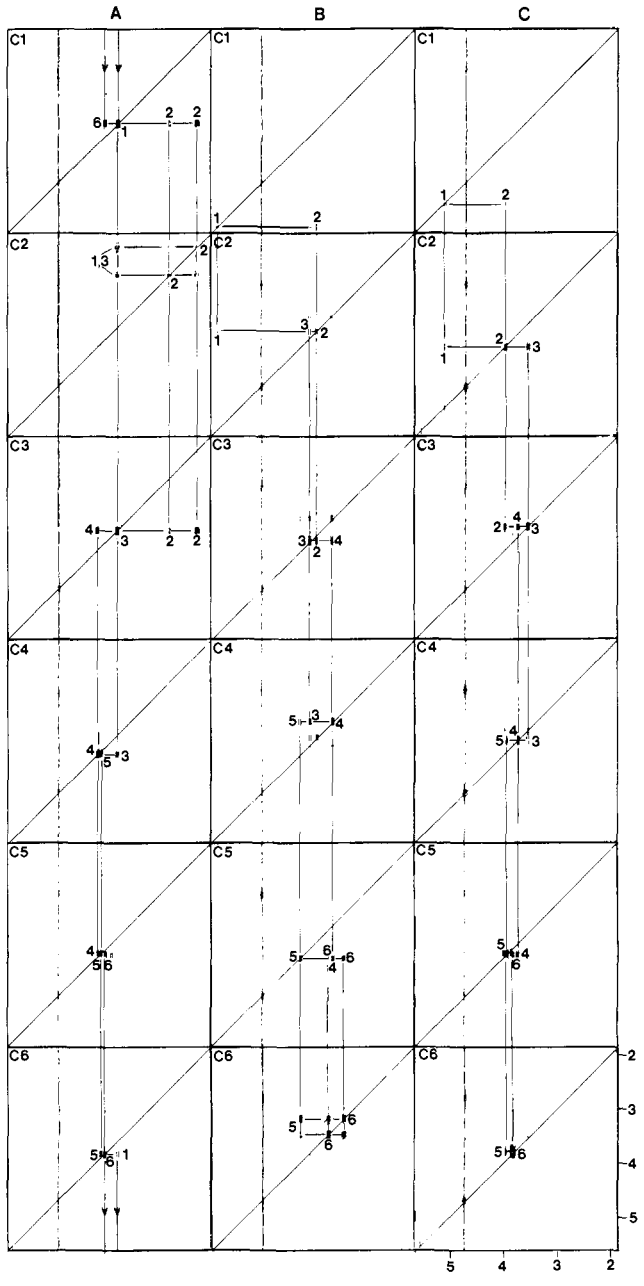

Figure 2. Individual planes (ω_2, vertical axis; ω_3, horizontal axis) of a 3D HMQC-COSY experiment at the ^{13}C frequencies (ω_1) corresponding to each of the carbon signals of 78 mM kanamycin A at ^{13}C natural abundance. The horizontal lines connect the protons that are scalar coupled, and the vertical lines connect the related planes. The peaks for the A, B, and C ring protons of kanamycin A are labeled as in the structure shown in Figure 1. The 3D data set was acquired on a Bruker AM500 NMR spectrometer as a series of 64 complex (t_1) ^{13}C shift-labeled homonuclear COSY experiments for which 64 complex t_2 values of 512 complex points (t_3) were obtained. A spectral width of ±1000 Hz was used in the ω_2 and ω_3 dimensions ±5000 Hz in the ω_1 dimension with the carrier placed in the center of all regions. A 1.8-s delay between scans and a 0.4-s delay following the BIRD pulse was employed. Four acquisitions and two dummy acquisitions were collected per t_3 experiment for a total experimental time of 74 h. The spectra were processed in the format of the FTNMR program of Dr. D. R. Hare with in house written software utilizing a CSPI minimap array processor interfaced to a Vax 8350 computer. Unshifted sine bell windows in ω_2 and ω_3 and a 90° shifted sine bell multiplied by a 45° shifted sine bell window function was applied in ω_1. After zero filling the final size of the 3D data set was 256 × 256 × 512 real points in ω_1, ω_2, and ω_3, respectively.

B of kanamycin A, the proton (H2) that is scalar coupled to H1 can easily be found in the plane corresponding to C1 (second column, top). The next step involves the selection of a plane (C2) that contains a diagonal peak (ω_2 = ω_3) at the frequency of H2

(6) Koyama, G.; Iitaka, Y.; Maeda, K.; Umezawa, H. *Tetrahedron Lett.* **1968**, 1875.
(7) Bax, A.; Subramanian, S. *J. Magn. Reson.* **1986**, *67*, 565.
(8) Shaka, A. J.; Keeler, J.; Frenkiel, T.; Freeman, R. *J. Magn. Reson.* **1983**, *52*, 335.
(9) Note that some of the planes contain additional patterns of proton signals (e.g., ring B—C3,C4; ring C—C4) which arise from overlap in the carbon (ω_1) dimension. The vertical noise band parallel to ω_2 in each of the planes corresponds to the residual HOD resonance.

and cross peaks corresponding to H1 and another proton (H3) that is scalar coupled to H2. This procedure is continued by selecting the protons that are scalar coupled to H3 from the plane (C3) that displays the proper pattern of proton signals (diagonal peak at H3, cross peak at H2). Ambiguities in the assignments which arise from protons resonating at the same frequency can be resolved in this experiment by editing the COSY data by the ^{13}C frequencies. For example, although the 1 and 3 protons of ring A have nearly identical chemical shifts, the shifts of the attached carbons (C1 and C3) are different. Thus, as shown in column 1 of Figure 2, the COSY responses involving the degenerate signals of H1 and H3 can be distinguished by their location in different planes (C1, H6-H1-H2; C3,H4-H3-H2).

Analogous to a two-dimensional heteronuclear relay experiment,[10] the 3D HMQC-COSY experiment provides relay information by correlating the chemical shifts of a carbon, the attached proton(s), and their scalar coupled partners. In contrast to the heteronuclear relay experiment, however, the 3D experiment uniquely defines the frequency of the relay spin.[2,3] This is important in cases where ^{13}C signals overlap such as C3 and C4 in ring B of kanamycin A. Since the relay spins (H3, H4) are uniquely defined in ω_2 in the 3D experiment, the H2-H3-H4 and H3-H4-H5 connectivity patterns can easily be distinguished (Figure 2).

In summary, heteronuclear 3D NMR spectroscopy is a useful method for resolving spectral overlap in all frequency domains. This is important for assigning spectra and elucidating the structures of complicated molecules. In addition, the increase in resolution afforded by this technique will help to automate peak-picking and assignment procedures and facilitate the extraction of J couplings (HMQC-COSY) and quantitative NOE information (HMQC-NOESY) used in the determination of three-dimensional structures.

Acknowledgment. We thank Dr. J. McAlpine for the sample of kanamycin A.

(10) (a) Bolton, P. H. *J. Magn. Reson.* **1982**, *48*, 336. (b) Bolton, P. H.; Bodenhausen, G. *Chem. Phys. Lett.* **1982**, *89*, 139.

The Use of 3D NMR in Structural Studies of Oligosaccharides

G. W. Vuister, P. de Waard, R. Boelens, J. F. G. Vliegenthart, and R. Kaptein*

Department of Chemistry, University of Utrecht Padualaan 8, 3584 CH Utrecht, The Netherlands

Received September 12, 1988

The three-dimensional structures of oligosaccharides derived from glycoproteins can be specified by the conformation of the glycosidic linkages, in particular the torsion angles ϕ and ψ and the additional torsion angle ω for 1-6 linkages.[1] Two-dimensional NOE spectra can provide interresidue proton distances, from which these torsion angles can be estimated. However, the small chemical shift dispersion of the sugar skeleton protons presents a major problem. In particular in the bulk region between 3 and 4 ppm there is a serious overlap of resonances. Often assignments can still be made in this region by multiple relayed COSY[2] or

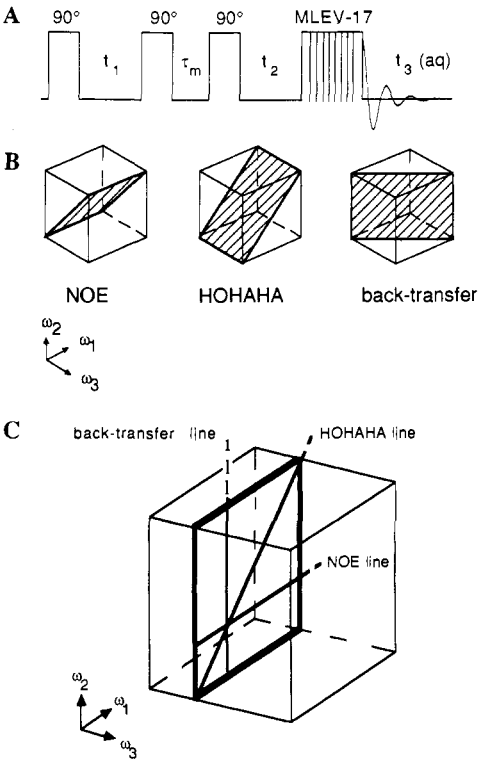

Figure 1. Nonselective 3D NOE-HOHAHA experiment. (A) Pulse sequence. (B) Cross diagonal planes in a 3D NOE-HOHAHA spectrum showing the NOE plane ($\omega_2 = \omega_3$), HOHAHA plane ($\omega_1 = \omega_2$), and back-transfer plane ($\omega_1 = \omega_3$). (C) Cross section perpendicular to the ω_3 axis. NOE, HOHAHA, and back-transfer lines result from intersection with the three planes indicated in part B.

by 1D or 2D homonuclear Hartmann-Hahn (HOHAHA) experiments[3] by using the shift dispersion of the anomeric protons. However, the NOE's involving protons of the bulk region would still be difficult to interpret.

The spectral resolution of the NMR methods can be increased by adding a third frequency domain.[4] Here we shall give an example of the application of 3D NMR to the diantennery asparagine-linked oligosaccharide **1**.

We will show that useful information on protons resonating in the bulk region can be extracted from a nonselective 3D NOE-HOHAHA experiment,[4f] which covers the full chemical shift range in all three dimensions.

The 3D NOE-HOHAHA can be visualized as a combination of a 2D NOE and a 2D HOHAHA or TOCSY experiment. The pulse sequence is shown in Figure 1A. The free induction decays (FIDs) are recorded in t_3 as a function of two independent evolution times t_1 and t_2. After 3D Fourier transformation of the FID's, the 3D frequency space can be represented in a cube with axes ω_1, ω_2, and ω_3. In the 3D spectrum obtained in this way a body diagonal ($\omega_1 = \omega_2 = \omega_3$) can be identified, containing magnetization not transferred during any of the mixing periods. Furthermore, intensity accumulates on the three cross-diagonal planes as shown in Figure 1B. The plane $\omega_2 = \omega_3$ (NOE plane) contains the magnetization transferred only during the NOE mixing period, whereas the plane $\omega_1 = \omega_2$ (HOHAHA plane) contains the magnetization transferred only during the isotropic mixing period of the MLEV-17 sequence. Finally, the plane $\omega_1 = \omega_3$ (back-transfer plane) contains magnetization transferred during the NOE mixing period from spin a to spin b and then

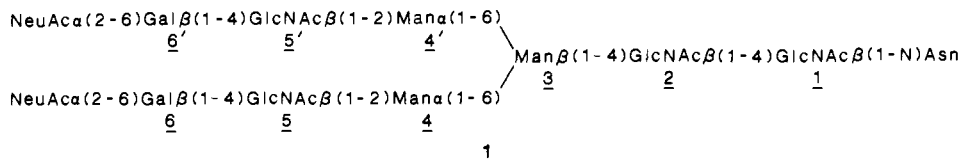

1